PAPER Special Section of 2004 International Symposium on Electromagnetic Compatibility

TDR Analysis of Electromagnetic Radiation from a Bend of Micro-Strip Line

Jianqing WANG[†a)] ***and*** **Osamu FUJIWARA**[†]**,** ***Members***

SUMMARY Discontinuity such as a bend in a micro-strip line is known as one of major radiation sources. The total radiation from the micro-strip line is, however, being generally investigated because of the difficulties in identifying the radiation from some specific location. In this paper, paying attention to the feature of TDR (Time-Domain Reflectometry) measurement, we made an attempt to extract the radiation only from the bend in a micro-strip line. Such an approach is useful in understanding its radiation mechanism. As a result, we found that the larger the bend angle is, the larger the radiation power becomes. The radiation power achieved 3.5% at maximum when the bending angle was 90° at the frequencies below 1 GHz. We also examined the validity of the TDR analysis in comparison with network analyzer measurement. We obtained the radiation power versus frequency from the measured scattering parameters, which exhibited a fair agreement with the TDR result.

key words: *TDR, micro-strip line, bend, radiation*

1. Introduction

Micro-strip lines are being widely used in printed circuit boards for digital signal transmission. The discontinuity such as a bend in a micro-strip line is regarded as one of major unwanted radiation sources. This is based on a consideration that a radiation can be attributed mainly to the point where the traveling-wave current is discontinuous, and such a consideration is often used to explain qualitatively the radiation mechanism [1], [2]. However, it is generally not easy to experimentally extract or identify the radiation from a specific bend in a micro-strip line, and therefore a full-wave analysis such as the method of moments or the finite difference time domain method is being used in the investigation [3]–[6]. In a full-wave analysis one has to make an effort to exclude the influences from the feeding point and the terminal where some discontinuities may exist. Otherwise the calculated radiation would come from not only the bend but also the other discontinuities. For example in [3], Lee and Hayakawa concluded that the 90° bend is the best with the least radiation loss, which is different from common understanding. In fact, however, their finding was not based on the radiation only from a single bend. Their finding was based on the total radiation including especially the connection parts between the connectors and the line. Such an approach is not effective in understanding the radiation characteristics only from a single bend.

In this paper, using time-domain reflectometry (TDR) measurement, we make an attempt to derive the radiation from a single bend in a micro-strip line. In a TDR waveform, it is easy to distinguish various reflections from time delays. This enables us to remove unwanted influences at the connection parts. An alternative is the use of thru-reflect-line (TRL) calibration technique in a network analyzer as described in [7]. Although it may provide a wider dynamic range or higher measurement precision, the calibration procedure is a considerable burden. From TDR measurement, we first describe a method to extract the reflected voltage waveform at the bend in time domain, and then we introduce a lossy admittance for expressing the radiation at the bend. By incorporating it into the transmission line model of the micro-strip line, we derive the voltage at the bend and then the radiated power from the bend. Such an approach is useful in understanding the radiation mechanism and radiation characteristics from a single bend. Its validity is examined by S-parameter measurement.

2. Measurement and Analysis

Figure 1 shows the basic principle of TDR. A step voltage with very fast rise time is input to the measuring object, and the response, i.e. the reflected voltage waveform is then recorded on an oscilloscope. From the reflected voltage waveform in time domain, we can identify and extract the part at a bend in a micro-strip line, for example. Moreover, due to the use of the very fast rise time for the step voltage, we can also derive wide-band frequency characteristics from the reflected voltage waveform based on Fourier transformation.

Figure 2 shows the structure of a micro-strip line with a bend. We used a glass-epoxy printed circuit board of $150 \times 75 \times 1.6$ mm, and fabricated the micro-strip line with a characteristic impedance of 50 Ω on one side of it. The micro-strip line was 150 mm ($l_1 + l_2$) long, and was

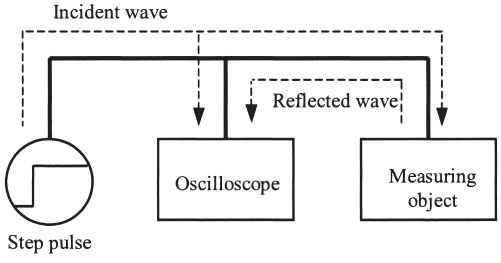

Fig. 1 Principle of TDR.

Manuscript received November 25, 2004.
Manuscript revised March 7, 2005.

[†]The authors are with the Graduate School of Engineering, Nagoya Institute of Technology, Nagoya-shi, 466-8555 Japan.
a) E-mail: wang@nitech.ac.jp

DOI: 10.1093/ietcom/e88–b.8.3207

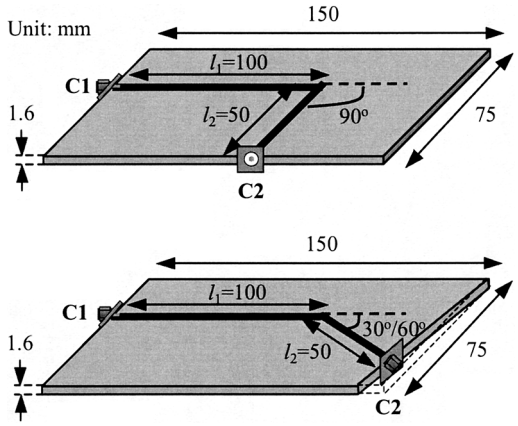

Fig. 2 Structure of a micro-strip line with a bend.

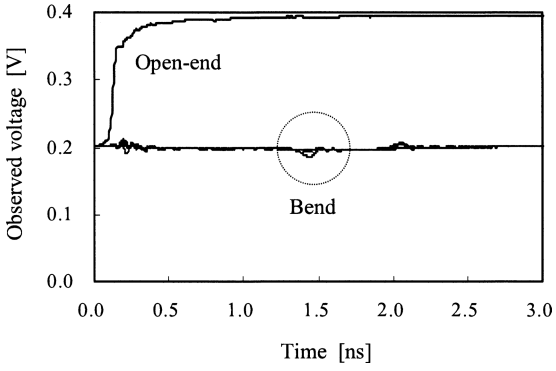

Fig. 3 Measured reflected voltage waveform in TDR.

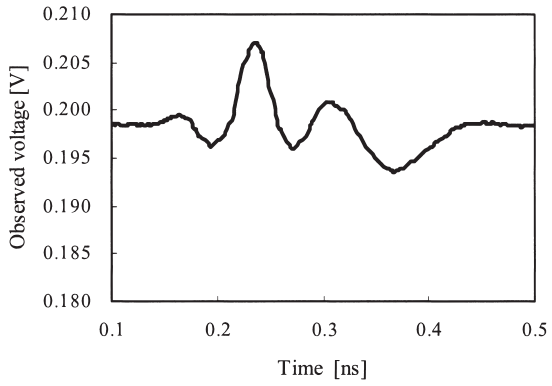

Fig. 4 Enlargement of reflected voltage waveform in the SMA connector on the input side to micro-strip line transition.

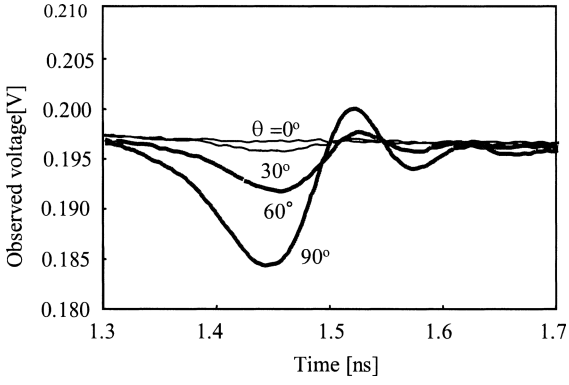

Fig. 5 Enlargement of reflected voltage waveform in the bend.

bended at the length of 100 mm (l_1) with various angles ($\theta = 0°, 30°, 60°, 90°$). We connected the TDR to one side of the micro-strip line via an SMA connector, and terminated the other side of the line with a 50 Ω (Z_o) load also via an SMA connector. To suppress the unwanted reflection at the connection between the SMA connector and the micro-strip line or the load, we soldered the SMA connector so that its internal conductor was a direct extension to the micro-strip line in the same direction. This yielded an irregular shape of the printed circuit board when the bending angle θ was 30° or 60°. The incident from the TDR (Agilent, TDR Module 54754 A) was a 0.2 V step voltage with a rise time of about 40 ps.

Figure 3 shows the reflected voltage waveform for the micro-strip line with a bend of 0°, 30°, 60° and 90°, respectively. Also shown in the figure is the reflected voltage for an open terminal, which was actually the incidence to the micro-strip line. Although we designed the micro-strip line to have both a characteristic impedance and a load of 50 Ω, we still found some reflections at the connector locations in Fig. 3. Since the time delay for the shortest separation of 50 mm was around 550 ps in the micro-strip line, each reflection waveform was extractable. The first voltage variation was due to the SMA connector on the input side, and the third voltage variation was due to the SMA connector on the load side. They should be attributed to the difficulty in making perfectly impedance matching between an SMA connector and a micro-strip line. The second voltage variation, i.e., the part in the circle, was due to the reflection at the bend. Figure 4 shows an enlargement of the extracted volatge waveform reflected at the input SMA connector, and Fig. 5 shows an enlargement of the reflected voltages for different bending angles. It was found that the influence of the discontinuity on the reflected voltage increases obviously for a larger bending angle. It should be noticed that the second voltage variation in Fig. 3 was not a pure reflected voltage at the bend for the incident step voltage. In fact, the incident step voltage was first reflected at the input SMA connector. Its transmitting voltage reached the bend and then was reflected again. The reflected voltage returned to the input SMA connector, and its transmitting voltage was recorded in the oscilloscope.

For a bend in a transmission line, it is known that a π-type LC circuit or a parallel capacitor can be used to model the reflection observed in the TDR voltage waveform [8]–[10]. However, it lacks a radiation loss so that it can not be used to investigate the radiation characteristics. In order to consider the radiation, we introduced a parallel admittance $Y_b(j\omega)$ (=$G_b(j\omega)$ + $jB_b(j\omega)$ where ω is the angular

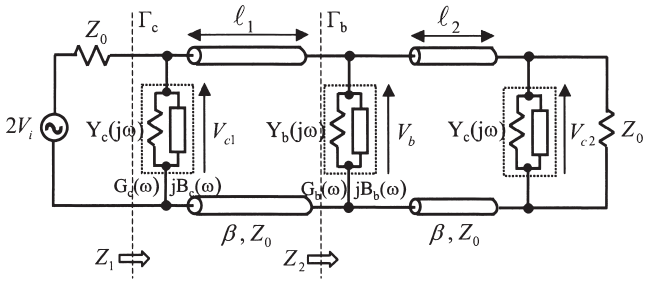

Fig. 6 Transmission line representation of a micro-strip line with a bend.

frequency) in place of a parallel capacitor. Similarly, for a coaxial cable to micro-strip line transition with an SMA connector, a T-type LC circuit is known as a good model [11], [12]. In view of the not-so-high frequencies to be investigated (below 1 GHz), we simplified the model also as a parallel admittance $Y_c(j\omega)$ (=$G_c(j\omega) + jB_c(j\omega)$). In such a way, we derived an equivalent transmission line representation, as shown in Fig. 6, for the micro-strip line with the bend, where V_i in the figure is the frequency-domain representation of the incident step voltage $v_i(t)$ of the TDR with respect to a 50 Ω load.

At first, let us consider the first voltage variation extracted in Fig. 4. We denoted it by $v_{rc}(t)$. The transmission line representation in Fig. 6 was then simplified as Fig. 7(a) because other influences apart from the input SMA connector did not appear in the first voltage variation. From Fig. 7(a) in the frequency domain, we obtained the admittance $Y_c(j\omega)$ as

$$Y_c(j\omega) = -\frac{2V_{rc}(j\omega)}{V_i(j\omega) + V_{rc}(j\omega)} \cdot \frac{1}{Z_o} = \frac{-2\int_{-\infty}^{\infty} \frac{dv_{rc}(t)}{dt} e^{-j\omega t} dt}{\int_{-\infty}^{\infty} \frac{dv_i(t)}{dt} e^{-j\omega t} dt + \int_{-\infty}^{\infty} \frac{dv_{rc}(t)}{dt} e^{-j\omega t} dt} \cdot \frac{1}{Z_o} \quad (1)$$

where $V_i(j\omega)$ and $V_{rc}(j\omega)$ are the frequency-domain representation of $v_i(t)$ and $v_{rc}(t)$, respectively, Z_o is the characteristic impedance of the micro-strip line, and Γ_c in Fig. 7(a) is the reflection coefficient (=$V_{rc}(j\omega)/V_i(j\omega)$) at $Y_c(j\omega)$. It should be noted that the employment of the differential calculus for $v_i(t)$ and $v_{rc}(t)$ is because that $v_i(t)$ has a direct voltage component and consequently its discrete Fourier transformation does not converge to a finite value. Differentiating $v_i(t)$ and $v_{rc}(t)$ with respect to time could exclude this problem.

Second, for the extracted voltage variation at the bend in Fig. 5, we denoted it by $v_{rb}(t)$. Figure 7(b) shows a transmission line representation for this case. Ignoring the loss and time delay of the micro-strip line, we have the voltage $V_{rbo}(j\omega)$ reflected from $Y_b(j\omega)$ as

$$V_{rbo}(j\omega) = \Gamma_b(1 + \Gamma_c)V_i(j\omega) = -\frac{2Z_o Y_b(j\omega)}{(2 + Z_o Y_c(j\omega))(2 + Z_o Y_b(j\omega))} \cdot V_i(j\omega) \quad (2)$$

where Γ_b is the reflection coefficients at $Y_b(j\omega)$. $V_{rbo}(j\omega)$

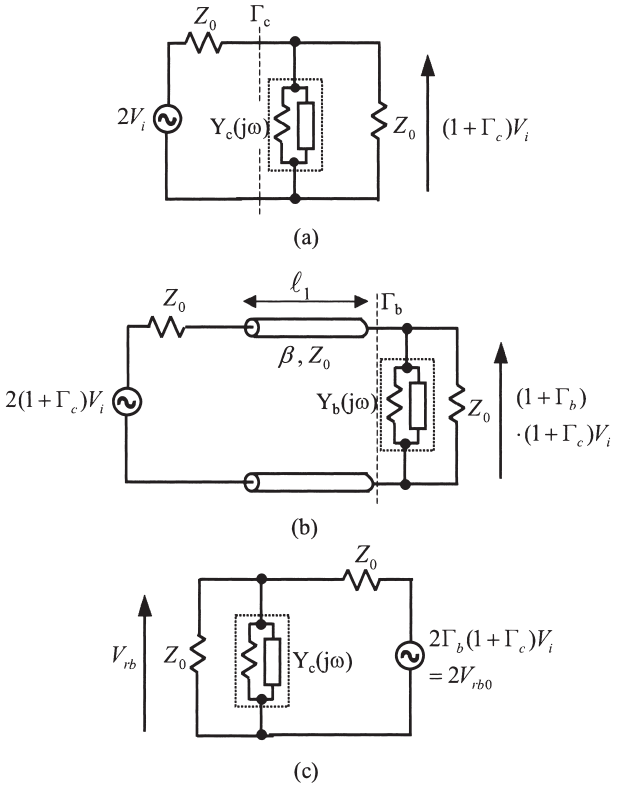

Fig. 7 (a) Circuit representation for the first voltage variation in the input SMA connector to micro-strip line transition. (b) Transmission line representation for the voltage variation in the bend. (c) Circuit representation for the observed voltage from the bend in the TDR.

acted actually as an incident voltage to $Y_c(j\omega)$. Its transmission line representation is shown in Fig. 7(c), where $V_{rb}(j\omega)$ is the frequency-domain representation of the observed voltage in the oscilloscope. Referring to Fig. 7(c), we have

$$V_{rb}(j\omega) = -\left[1 + \frac{V_{rc}(j\omega)}{V_i(j\omega)}\right]^2 \frac{Z_o}{Z_o + 2/Y_b(j\omega)} \cdot V_i(j\omega). \quad (3)$$

Solving the above equation, we have

$$Y_b(j\omega) = -\frac{2\,V_{rb}(j\omega)}{V_{rb}(j\omega) + \left[1 + V_{rc}(j\omega)/V_i(j\omega)\right]^2 V_i(j\omega)} \cdot \frac{1}{Z_o}. \quad (4)$$

In deriving $Y_c(j\omega)$ and $Y_b(j\omega)$ from the TDR-extracted voltage waveforms, we employed the FFT algorithm for Fourier transformation. For both $v_{rc}(t)$ and $v_{rb}(t)$, we measured them with a sampling interval of 1.953 ps. We extracted them with a rectangular gate having a time width of 400 ps at their corresponding locations. We shifted the extracted waveforms of the reflected voltages along the time axis to have the same starting time as the incident voltage $v_i(t)$ in order to remove the influence of time delay, and then extended the total measuring time by adding data with a

value equal to the initial voltage (nearly 0.2 V). This process yielded a total data number of 8192 for each waveform in the time domain and a resolution of 62.5 MHz in the frequency domain.

After obtaining $Y_c(j\omega)$ and $Y_b(j\omega)$, we calculated the voltages $V_{c1}(j\omega)$, $V_b(j\omega)$ and $V_{c2}(j\omega)$ using a transmission line theory for the equivalent representation in Fig. 6. Letting by $Z_1(j\omega)$ and $Z_2(j\omega)$ be the input impedances looking toward the righ-hand side as shown in Fig. 6, we derived the radiated power from the bend as follows:

$$\begin{aligned} P_b(\omega) &= |V_b(j\omega)|^2 Re[Y_b(j\omega)] \\ &= 4\left|\frac{Z_1(j\omega)Z_2(j\omega)}{[Z_o + Z_1(j\omega)][Z_2(j\omega)\cos(\beta l_1) + jZ_o\sin(\beta l_1)]}\right|^2 \\ &\quad \times |V_i(j\omega)|^2 Re[Y_b(j\omega)] \end{aligned} \tag{5}$$

where β is the phase constant and was determined from the physical dimensions of the micro-strip line and the electric properties of the dielectric layer [13]. For the input impedances of $Z_1(j\omega)$ and $Z_2(j\omega)$, we have

$$Z_1(j\omega) = Z_0 \times \frac{Z_2/Z_o + j\tan(\beta l_1)}{(1 + Z_2Y_c) + j(Z_2/Z_o + Z_oY_c)\tan(\beta l_1)} \tag{6}$$

and

$$\begin{aligned} Z_2(j\omega) &= Z_0 \\ &\times \frac{1 + j(1 + Z_oY_c)\tan(\beta l_2)}{(1 + Z_oY_c + Z_oY_b) + j(1 + Z_oY_b + Z_o^2Y_cY_b)\tan(\beta l_2)} \end{aligned} \tag{7}$$

where Y_c and Y_b indicate $Y_c(j\omega)$ and $Y_b(j\omega)$, respectively, for simplicity.

Similarly, we also derived the radiated power from the two SMA connectors as follows:

$$P_{c1}(\omega) = |V_{c1}(j\omega)|^2 Re[Y_c(j\omega)] \tag{8}$$

$$P_{c2}(\omega) = |V_{c2}(j\omega)|^2 Re[Y_c(j\omega)]. \tag{9}$$

The total radiated power from the micro-strip line was then obtained from

$$P_r(\omega) = P_b(\omega) + P_{c1}(\omega) + P_{c2}(\omega). \tag{10}$$

3. Result and Discussion

Figure 8 shows the admittance $Y_c(j\omega)$ for the SMA connector to micro-strip line transition in the frequency range up to 1 GHz, and Fig. 9 shows $Y_b(j\omega)$ for the bend. They were derived based on the TDR measurement as described above. As a result, we found that the susceptance component of $Y_c(j\omega)$ was inductive, while the susceptance components of $Y_b(j\omega)$ were capacitive for all bending angles. The capacities were about 0.03, 0.06 and 0.21 pF for 30°, 60° and 90° bends, respectively, by fitting them with $2\pi fC$ (f: frequency, C: capacitance). This was identical to the finding obtained in [10]. On the other hand, the conductance of the admittance $Y_b(j\omega)$ exhibited an increasing feature with the frequencies and bending angles.

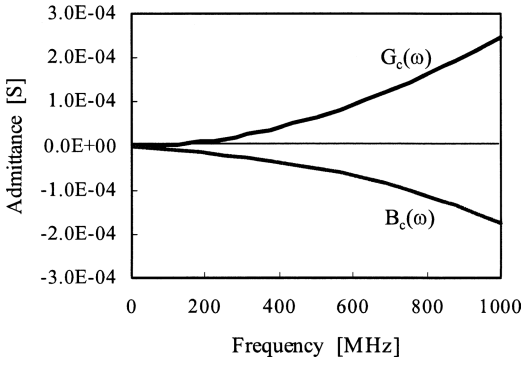

Fig. 8 Equivalent admittance derived from TDR versus frequency for the SMA connector to micro-strip line transition.

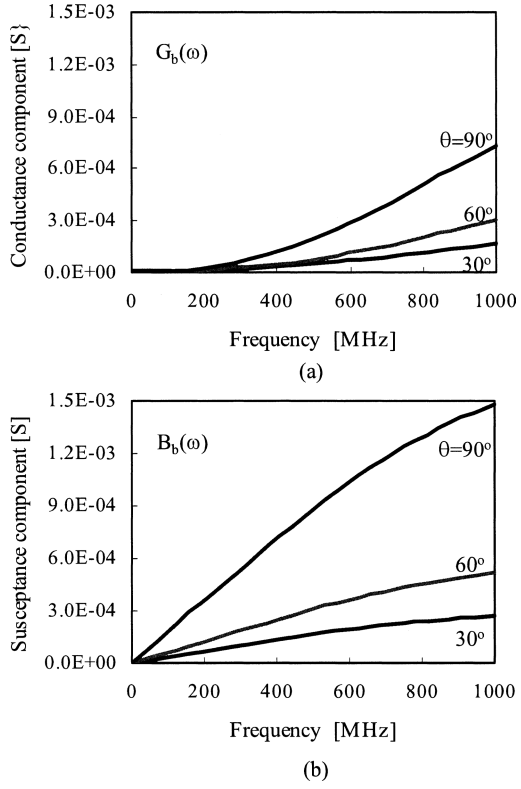

Fig. 9 Equivalent admittance derived from TDR versus frequency for the bends. (a) Conductance component, (b) susceptance component.

Figure 10 shows the radiated power at the bends calculated from Eq. (5), which was normalized to the incident power $P_i = |V_i|^2/50$. As can be seen, the larger the bending angle is, the larger the radiated power becomes. The radiated power achieved 3.5% at maximum when the bending angle was 90° at the frequencies below 1 GHz. The finding showed that a small bend is better from the point of view of radiation suppression, and suggested that the conclusion in [3], i.e., a 90° bend with a least radiation does not hold when considering the radiation only from a single bend.

To verify the validity of the TDR analysis, we em-

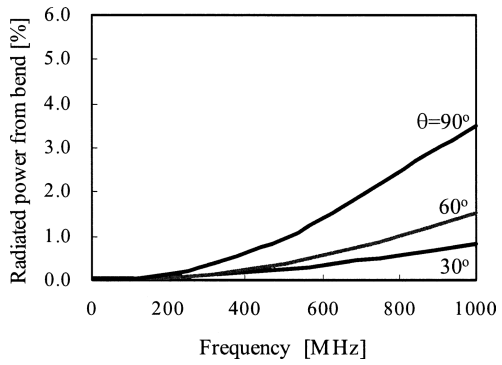

Fig. 10 Relative radiated power from the bends based on TDR analysis versus frequency.

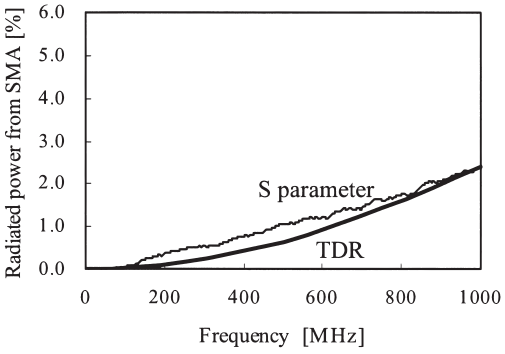

Fig. 11 Comparison of the total radiated power between TDR analysis and S-parameter measurement for a micro-strip line without a bend.

ployed a network analyzer and measured the S-parameters. We connected the two ports of the network analyzer to the two sides of the micro-strip line, and obtained the reflection coefficient S_{11} and the transmission coefficient S_{21}. Under the assumption that the loss of micro-strip line itself is insignificant in the investigated frequency band, we derived the radiated power, normalized to the incident power $P_i(\omega)$, from

$$\frac{P_r(\omega)}{P_i(\omega)} = 1 - |S_{11}|^2 - |S_{21}|^2. \tag{11}$$

Figure 11 shows the relative radiated power $P_r(\omega)$ versus frequency between the TDR analysis and the S-parameter measurement for a straight line (without a bend), and Fig. 12 shows that for bending angles of 30° and 90°. The radiated power in Fig. 11 was calculated only from the two discontinuities at the SMA connectors. It exhibited a fair agreement with the S-parameter-measured one, although the measured result was somewhat larger at lower frequencies. Comparing the TDR-derived total radiated power with S-parameter-measured one for a bend in Fig. 12, we found an acceptable agreement between them. The deviation at lower frequencies should still be attributed to the SMA connector to micro-strip line transitions, and the deviation around 1 GHz may be due to the ignored loss of the micro-strip line itself. In total, the agreement between the

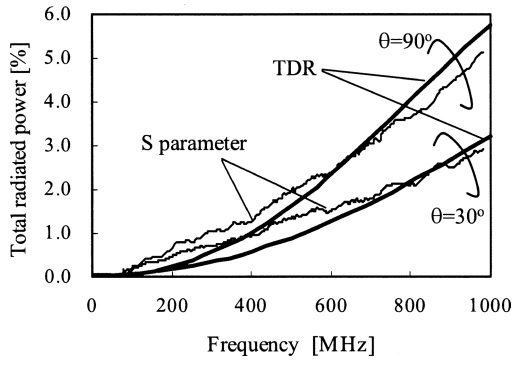

Fig. 12 Comparison of the total radiated power between TDR analysis and S-parameter measurement for a micro-strip line with a bend.

TDR-derived and S-parameter-measured results in the both cases without and with a bend supported the validity of our approach.

4. Conclusion

Although a bend in a micro-strip line is known as one of major radiation sources, its radiation characteristics are still not well understood because of the difficulty in extracting the radiation only from the bend in experiment. Paying attention to the feature of TDR measurement, in this study we have attempted to extract the radiation only from the bend. We first extracted the reflected voltage waveform at the bend in time domain via TDR measurement, and then we introduced a lossy admittance for expressing the radiation at the bend. By incorporating it into the transmission line model of the micro-strip line, we have derived the radiated power from the bend. As a result, we have found that the larger the bending angle is, the larger the radiated power becomes. The radiated power achieved 3.5% at maximum when the bending angle was 90° at the frequencies below 1 GHz. To confirm the validity of the TDR analysis by S-parameter measurement, we have compared the total radiated power versus frequency between the TDR analysis and the S-parameter measurement. As a result, we have found a fair agreement between them, which supports the validity of this approach.

The future subject is to extend the method to multi-bends and higher frequencies.

References

[1] R.E. Collin and F.J. Zucker, Antenna Theory, Chapter 21, McGraw-Hill, New York, 1969.

[2] T. Nakamura, N. Okochi, S. Yokokawa, and R. Sato, "Radiation from a bend of transmission line," IEICE Trans. Commun. (Japanese Edition), vol.J70-B, no.2, pp.261–268, Feb. 1987.

[3] S. Lee and M. Hayakawa, "A study on the radiation loss from a bent transmission line," IEEE Trans. Electromagn. Compat., vol.43, no.4, pp.618–621, Nov. 2001.

[4] M. Takahashi, M. Takahashi, and M. Abe, "Radiation electromagnetic waves suppressed by the curve shape of microstrip line," IEICE Trans. Electron. (Japanese Edition), vol.J82-C-I, no.9, pp.561–569,

Sept. 1999.
[5] T. Shiokawa, "FDTD analysis of the transmission/radiation characteristics of 90° bent transmission line," IEICE Trans. Commun. (Japanese Edition), vol.J86-B, no.7, pp.1070–1080, July 2003.
[6] H. Wang, Y. Ji, T.H. Hubing, J.L. Drewniak, T.P. Van Doren, and R.E. DuBroff, "Experimental and numerical study of the radiation from microstrip bends," Proc. IEEE Inter. Symp. on Electromagn. Compat., pp.739–741, Washington D.C., Aug. 2000.
[7] S. Vandenberghe, D. Schreurs, G. Carchon, B. Nauwelaers, and W. De Raedt, "Characteristic impedance extraction using calibration comparison," IEEE Trans. Microw. Theory Tech., vol.49, no.12, pp.2573–2579, Dec. 2001.
[8] B. Easter, "The equivalent circuit of some microstrip discontinuities," IEEE Trans. Microw. Theory Tech., vol.23, no.8, pp.655–660, Aug. 1975.
[9] J.-M. Jong, B. Janko, and V. Tripathi, "Equivalent circuit modeling of interconnects from time-domain measurement," IEEE Trans. Compon. Hybrids Manuf. Technol., vol.16, no.1, pp.119–126, Feb. 1993.
[10] N. Kuramata, K. Baba, and T. Takagi, "Analysis of pulse response characteristics for bended line," IEICE Technical Report, EMCJ93-42, Oct. 1993.
[11] A.G. Chapman and C.S. Aitchison, "A broad-band model for a coaxial-to-stripline transition," IEEE Trans. Microw. Theory Tech., vol.28, no.2, pp.130–136, Feb. 1980.
[12] M.L. Majewski, R.W. Rose, and J.R. Scott, "Modeling and characterization of microstrip-to-coaxial transitions," IEEE Trans. Microw. Theory Tech., vol.29, no.8, pp.799–805, Aug. 1981.
[13] C.R. Paul, Introduction to Electromagnetic Compatibility, pp.265–274, John Wiley & Sons, New York, 1992.

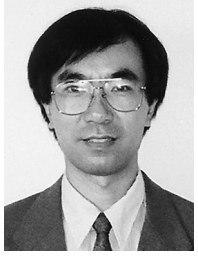

Jianqing Wang received the B.E. degree in electronic engineering from Beijing Institute of Technology, Beijing, China, in 1984, and the M.E. and D.E. degrees in electrical and communication engineering from Tohoku University, Sendai, Japan, in 1988 and 1991, respectively. He was a Research Associate at Tohoku University and a Research Engineer at Sophia Systems Co., Ltd., prior to joining the Nagoya Institute of Technology, Nagoya, Japan, in 1997, where he is currently a Professor. His research interests include electromagnetic compatibility, bioelectromagnetics and digital communications.

Osamu Fujiwara received the B.E. degree in electronic engineering from Nagoya Institute of Technology, Nagoya, Japan, in 1971, and the M.E. and the D.E. degrees in electrical engineering from Nagoya University, Nagoya, Japan, in 1973 and in 1980, respectively. From 1973 to 1976, he worked in the Central Research Laboratory, Hitachi, Ltd., Kokubunji, Japan, where he was engaged in research and development of system packaging designs for computers. From 1980 to 1984 he was with the Department of Electrical Engineering at Nagoya University. In 1984 he moved to the Nagoya Institute of Technology, where he is presently a professor. His research interests include measurement and control of electromagnetic interference due to discharge, bioelectromagnetics and other related areas of electromagnetic compatibility. Dr. Fujiwara is a member of the IEE of Japan and of the IEEE.